electronics

MDPI

Article

Effectiveness of Fuzzy Logic Controller in Maintaining Stability of Digital Twin-Enabled Offshore Wind Farm (OWF) Integrated with HVDC Grid

Yamini Gaddam and Mohd. Hasan Ali *

Electrical and Computer Engineering, Herff College of Engineering, University of Memphis, 3720 Alumni Ave, Memphis, TN 38111, USA; ygaddam@memphis.edu
* Correspondence: mhali@memphis.edu

Abstract

Offshore wind farms are increasingly and rapidly expanding due to their ability to harness strong and consistent wind energy resources. Large offshore wind farms are connected to mainland grids through High-Voltage Direct Current (HVDC) technology. However, offshore wind farms can often experience disturbances related to sudden wind changes, voltage drops/dips, faults related to converter switching, and unbalanced grid conditions which affect both the HVDC operation and wind turbine output. As a result, there is a growing need for more advanced and reliable modeling and monitoring tools. Moreover, traditional proportional-integral (PI) controllers are widely applied in wind turbines and HVDC systems due to their simple structure, easy implementation, and reliability. However, PI controllers perform poorly under non-linear and abnormal/fast-changing conditions, especially during sudden drops in wind power and grid faults. With this background, this paper first develops a digital twin model of an offshore wind farm that enables remote operation and monitoring of individual wind turbines. Also, an artificial intelligence (AI)-based controller, namely a fuzzy logic controller (FLC), is proposed to maintain transient stability of a full digital twin-based offshore wind farm connected to the HVDC grid under fault conditions. The effectiveness of the proposed FLC is demonstrated by considering a digital twin-enabled 700 MW offshore wind farm. The performance of the proposed FLC has been compared with that of the PI controller. Simulations performed by the MATLAB/Simulink software show that during the moderate voltage dip at 15 s, the PI controller experienced a 29.8% power reduction with a recovery time of approximately 9 s, whereas the FLC reduced the power drop to 23.1% and recovered within 6 s. During the severe converter disturbance at 15 s, the PI controller recorded a 36.9% power reduction compared to 23.4% for the FLC. Similarly, during the short-duration turbulence at 15 s, the PI controller exhibited a 36.73% power drop and recovered in approximately 7 s, while the FLC limited the power reduction to 19.17% and recovered within 5s. Overall, the FLC provided improved voltage stability, faster recovery, reduced oscillations, and superior fault ride-through capability compared with the conventional PI controller, demonstrating its effectiveness for digital twin-enabled offshore wind farm application.

Keywords: offshore wind farm; digital twin; fuzzy logic controller; power system stability

Academic Editor: Cristina Ventura

Received: 18 May 2026
Revised: 17 June 2026
Accepted: 20 June 2026
Published: 24 June 2026

1. Introduction

Offshore wind farms are increasingly and rapidly expanding due to their ability to harness strong and consistent wind energy resources. Offshore wind energy has become a crucial source of renewable energy that capitalizes on strong and steady wind resources [1,2]. Offshore wind energy is also playing an increasingly important role in the global energy transition as countries seek to reduce carbon emissions and increase the share of renewable energy in their electricity generation mix. Many national energy strategies and net-zero roadmaps identify offshore wind as a key technology for achieving long-term decarbonization targets due to its large-scale generation capability and high-capacity factors [3,4]. Compared to onshore wind farms, offshore wind farms are often stronger and more consistent and can support large-scale electricity production. However, there are some system-level challenges associated with offshore wind farms that are worthy of note. Despite the several advantages, these shortcomings make the integration of offshore wind farms into other existing power systems technically and operationally challenging. High-Voltage Direct Current (HVDC) technology is used to efficiently connect large offshore wind farms to mainland grids [3]. Besides meeting the need for long transmission lines, the associated per-kilometer costs, including capital and running costs, of HVDC are significantly lower than HVAC. In addition, the lack of reactive power and skin effects in HVDC systems reduces or limits losses in power delivery. Furthermore, HVDC technology can allow for connection with two unsynchronized power systems, and its flexible power control can stabilize low-inertia systems.

Recent studies have shown that voltage source converter (VSC)–HVDC systems are particularly suitable for offshore wind integration because they provide independent control of active and reactive power, support weak-grid operation, and improve fault ride-through performance. Besides conventional VSC-HVDC and LCC-HVDC technologies, recent research has explored hybrid HVDC architectures and controllable line-commutated converter (CLCC) systems [5]. CLCC-HVDC combines the high-power transmission capability of conventional line-commutated converters with improved controllability during fault conditions. According to the research, CLCC-based hybrid HVDC systems can enhance fault ride-through performance and improve operational flexibility for large-scale renewable energy integration. These developments further demonstrate the continuing evolution of HVDC technology for offshore wind applications and future low-carbon power systems. Consequently, VSC-HVDC technology has become the preferred solution for connecting large offshore wind farms located far from onshore transmission networks [6,7].

However, offshore wind farms can often experience disturbances related to sudden wind changes, voltage drops/dips, faults related to converter switching and unbalanced grid conditions which affect both the HVDC operation and wind turbine output. As a result, there is a growing need for more advanced and reliable modeling and monitoring tools such as digital twin technology. Digital twin technology is simply a digital representation of a physical asset. With the continuous growing of wind turbines in size and increased deployment offshore, their operation and maintenance become challenging. Due to distance, onsite assessment and maintenance of offshore wind turbines in remote places is a big challenge compared to onshore wind turbines. Hence, real-time monitoring of the offshore wind farm (OWF)–HVDC system is essential to facilitate timely detection, diagnosis and elimination of faults based on sensor data. However, it is often challenging to extract valuable data/information and construct insights from heterogeneous and dynamic sensor data [4]. A digital twin can facilitate the management of wind farms in hostile environments and potentially increases safety and reduces operational and maintenance costs [8]. Also, it can predict the OWF-HVDC physical system's remaining life based on virtual operation such as maintenance as well as on state monitoring and hence offer viable suggestions for effective operation and management [9]. The data that the digital twin monitors in real time provides is the basis for its anomaly detection/diagnosis and fault identification [10]. As such, a digital twin is an essential and powerful tool in diagnosing, describing, predicting and decision making in the installation and operation and maintenance of offshore wind turbines.

It is noteworthy that when a fault occurs in the OWF system, which can be generator or converter faults, sudden turbine power drops, grid frequency instabilities, communication failures or grid voltage dips, the stability and efficiency of an offshore wind farm is significantly affected [11]. For instance, the occurrence of an offshore DC or AC fault and the subsequent sudden reduction in voltage might result in an overcurrent in offshore HVDC converter stations [7]. Fault ride-through strategies like the current-voltage droop method mitigate faults by modifying the output voltage reference based on offshore three-phase current readings/measurements [12]. Research shows that Proportional Integral (PI) controllers are widely used in wind energy and voltage source converter (VSC)–HVDC systems as a control technique because they are simple, robust and easy to adjust/tune [10,11]. In VSC-HVDC systems, PI controllers are used as an outer DC link voltage control and an inner current control [12]. These controllers form the main controller unit of a multi-terminal HVDC transmission network and facilitate the regulation of the DC link voltage and power transmission/flow. However, studies show that during faults and disturbances, such as sudden voltage dips, PI controllers often show slowed recovery. Despite PI controllers' reliability, they show weakness in dealing with non-linear converter behavior and fast disturbances [13]. PI controllers respond poorly during rapidly changing wind conditions, produce voltage/power overshoot during abrupt system changes and lack adaptability under disturbances or fault events.

To overcome the limitations of PI controllers, artificial intelligence (AI)-based controllers, such as a fuzzy logic controller (FLC), can be appropriate to maintain transient stability of OWFs. The specific feature of FLCs is that they do not require an exact mathematical model but instead use human-like reasoning/expert knowledge and linguistic rules. FLCs are considered robust and intelligent adaptive tools designed for complex non-linear systems and require the selection/defining of linguistic variables, membership functions, a preferred defuzzification strategy and the inference method.

Based on the above background, this paper first develops a digital twin model of an offshore wind farm that enables remote operation and monitoring of individual wind turbines and the associated HVDC transmission system. Then a fuzzy logic controller (FLC) is proposed to maintain transient stability of a full digital twin-based offshore wind farm connected to the HVDC grid under fault conditions. Although previous studies have investigated digital twins and intelligent controllers separately, limited research has combined a digital twin framework with fuzzy logic-based transient stability enhancement for offshore wind farms connected through VSC-HVDC systems. The proposed FLC differs from conventional PI control by using the voltage error and change of error as adaptive inputs processed through linguistic rules rather than relying solely on fixed controller gains. The main novelty of this work is the integration of a digital twin environment with an adaptive FLC for fault monitoring and transient stability improvement in a 700 MW OWF-HVDC system. The effectiveness of the proposed FLC is demonstrated by comparing its performance with that of a conventional PI controller under multiple fault conditions.

In this work, three fault scenarios such as a moderate voltage drop, severe converter disturbance, and a short duration dip from wind turbulence have been considered in the DT model to compare the performance of the PI controller and FLC. By allowing for high-fidelity modeling of wind turbines, converters, controllers and grid systems, MATLAB/Simulink R2024a (MathWorks, Natick, MA, USA) has been used in DT development in this work [14]. By integrating MATLAB/Simulink modeling, rule-based logic and external excel data, the DT creates a realistic simulation environment.

In summary, the key contributions of this paper are as follows.

(i) It develops a digital twin model for the monitoring, fault analysis, and performance evaluation of an offshore wind farm connected to an HVDC grid.
(ii) It develops an adaptive fuzzy logic controller based on voltage error and change of error inputs to improve transient stability during fault conditions.
(iii) It evaluates and compares the performance of the proposed FLC and a conventional PI controller under multiple offshore wind farm fault scenarios.
(iv) It demonstrates the effectiveness of integrating digital twin technology with intelligent control for improved fault ride-through capability and system recovery.

This paper is organized as follows. Section 2 describes the offshore wind farm and its digital twin model. Section 3 explains the design of the proposed fuzzy logic controller. Section 4 provides simulation results and discusses the interpretation of the simulation results, digital twin benefits, and control system implications. Section 5 provides conclusions. Also, limitations and future work are discussed at the end of the Conclusions.

2. Offshore Wind Farm and Its Digital Twin Model

2.1. Offshore Wind Farm System

Figure 1 shows the circuit diagram of the offshore wind farm connected to the onshore grid via a VSC-HVDC transmission link. The power that the 700 MW OWF generates is converted to DC at the offshore converter station, transmitted through the HVDC link and converted back to AC at the onshore converter station before being injected into the grid. Table 1 shows the system parameters used in this study. Also, Table 2 provides an explanation on each component of the system in Figure 1.

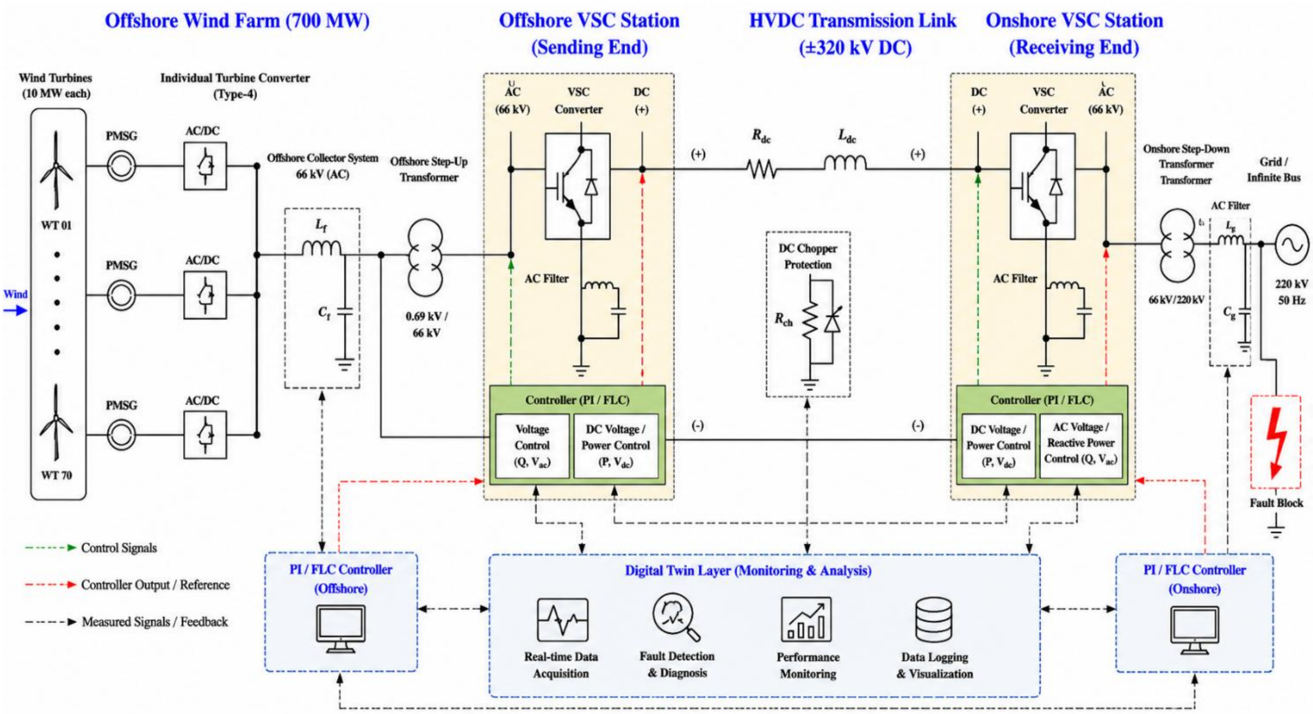

Figure 1. Circuit diagram of offshore wind farm with control strategy.

Table 1. System parameters used in this study.

Parameter	Symbol	Value	Unit
Total Wind Farm Capacity	Pwf	700	MW
Turbine Rated Power	Pt	10	MW

Table 1. *Cont.*

Parameter	Symbol	Value	Unit
Number of Turbines	N	70	–
Generator Type	–	PMSG (Type-4)	–
Turbine Rated Voltage	Vt	0.69	kV (AC)
Collector System Voltage	Vcol	66	kV (AC)
HVDC Link Voltage	Vdc	±320	kV (DC)
DC Cable Resistance	Rdc	0.12	Ω
DC Cable Inductance	Ldc	0.35	mH
DC Chopper Resistance	Rch	50	Ω
Onshore Grid Voltage	Vgrid	230	kV (AC)
Grid Frequency	F	50	Hz
Filters (AC Filter)	Lf/Cf	2 mH/50 μF	–
Smoothing Reactor	Lg	10	mH

Table 2. Explanation of components.

Component	Explanation
Wind Turbines & PMSG (Type-4)	Capture wind energy and convert it to AC power using permanent-magnet synchronous generators.
Rotor side converter (RSC)	Controls rotor speed, frequency, and active power output.
Grid side converter (GSC)	Controls generator terminal voltage, power factor, and reactive power.
Individual Turbine Converter (AC/DC)	Back-to-back converter converting variable-frequency AC to DC and controlling active/reactive power.
Offshore Step-Up Transformer	Steps voltage from 0.69 kV to 66 kV.
Offshore VSC Station (Sending End)	Converts AC (66 kV) to DC (±320 kV) and controls DC voltage and power flow.
HVDC Transmission Link	Bipolar DC cable with series R and L; DC chopper provides over-voltage protection.
Onshore VSC Station (Receiving End)	Converts DC back to AC (66 kV) and regulates AC voltage and reactive power.
Onshore Step-Down Transformer	Steps voltage from 66 kV to 230 kV.
Onshore AC System Filters	Filters harmonics before connecting to the grid.
Grid/Infinite Bus	Represents the strong onshore power system.
Fault Block	Applies fault scenarios such as voltage dips or converter disturbances.
Controllers (PI/FLC)	Generate control signals for converter regulation during normal and fault conditions.

2.2. Digital Twin of Offshore Wind Farm

Digital twins virtually represent and replicate physical object/s in a virtual environment. Digital twins involve integrating three distinct components, i.e., the physical space, the virtual space, and the communication between these two spaces [15]. By continuously receiving real-time data from internet-of-things (IoT) sensors and utilizing artificial intelligence (AI), they mirror their real-world counterpart's behavior to allow engineers to simulate, analyze, and optimize performance without risking the actual asset [16]. Digital twins have demonstrated significant potential across various industries, garnering considerable attention from both industrial and academic sectors [17]. Figure 2 illustrates the normal digital twin block diagram, demonstrating the automatic bidirectional exchange of data between the physical system and digital/simulation model.

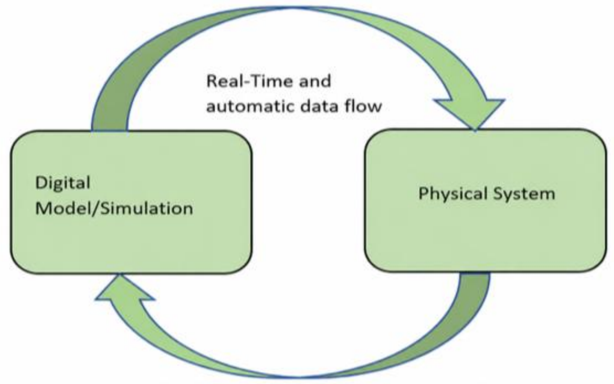

Figure 2. Basic digital twin block diagram.

With the continuous growing of wind turbines in size and increased deployment offshore, their operation and maintenance become challenging. Due to distance, onsite assessment and maintenance of offshore wind turbines in remote places is a big challenge compared to onshore wind turbines. That is why in this work a digital twin has been developed for the OWF shown in Figure 1. A synthetic dataset was generated in Excel to represent realist OWF behavior because real SCADA data from offshore wind farms were not available. Thus, future research should focus on integrating real SCADA data from offshore wind farms and other additional non-linear effects like converter switching. The synthetic dataset was generated in Excel based on realistic operating conditions of an offshore wind farm. Wind speed values were varied within a practical offshore range (3–25 m/s) to represent normal wind fluctuations. Power output was estimated using a simplified wind turbine–power relationship, where power increases with wind speed and is limited at the rated capacity of 700 MW. Voltage and frequency were kept around their nominal values (1.0 pu and 50 Hz) with small variations to reflect normal grid behavior.

Fault events were not random but were added at specific simulation times to test system performance under controlled conditions. The fault event signal was defined as a binary input (0 or 1), where "1" indicates the presence of a fault. Overall, the dataset was designed to realistically represent offshore wind farm behavior while allowing for testing of the two controllers under fault conditions. The variables for the dataset included time (s), wind speed (m/s), power generated (MW), power set point (MW), fault event signal (0/1), voltage (pu) and frequency (Hz). The dataset was used to simulate a 700 MW OWF with varying conditions.

Figure 3 illustrates the interaction between the physical OWF-HVDC system and the digital twin layer developed in MATLAB/Simulink. The digital twin continuously receives and processes measured system variables, including voltage, current, power, and frequency, for fault detection, controller action, and system monitoring [18]. The PI and FLC controllers generate the decision/control signals which are fed back to the physical system to enhance/improve stability during fault conditions.

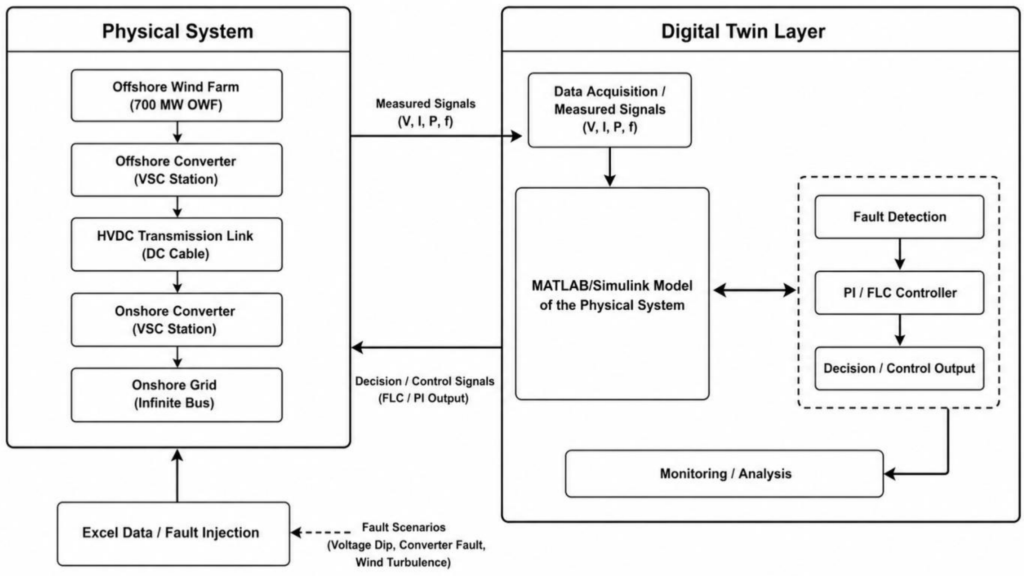

Figure 3. Digital twin simulation workflow for OWF-HVDC system.

2.2.1. Fault Induction

Three fault scenarios were deliberately created in the DT model to compare the performance of the two controllers, PI and FLC. In Simulink, these fault scenarios are modeled by feeding the fault event into the two controllers' logic. As such, when fault_event = 1, the controllers enter a Fault Ride-Through mode, which results in a reduction in the active power set point, a modification of the current and the application of any other designed responses.

2.2.2. Fault Detection Logic

Fault detection is a crucial component of DT as it guides operators on when to switch controllers and trigger protective measures. DTs facilitate predictive failure and fault diagnosis and execution of what-if scenarios to analyze the system response to parametric and operational parameters [19,20]. Generally, a fault was detected when voltage was <0.8 pu, frequency was <49.5 Hz and power dropped to >15%. Consequently, when a fault is detected, the DT fault logic sets fault_event = 1, which activates the controllers' FRT mode.

2.2.3. Data Logging and Analysis

During the simulation, several signals, including generated power (MW), power set point (MW), voltage (pu), frequency (Hz), controller adjustment/output (ΔP) and fault event signal, were logged to assess the two controllers' performance during normal and fault scenarios. These logged signals were then fed back to an Excel file to mimic the digital twin's feedback loop. Consequently, the power drop magnitude, recovery time, overshoot or oscillations after fault event steady-state errors were analyzed.

3. Design of Proposed Fuzzy Logic Controller

FLCs are designed to be more adaptive and resilient under fault events or disturbances. Research shows that unlike PI controllers, FLCs can handle system non-linearity based on linguistic if-then rules, is easy to implement as it has a simple design requirement, is less sensitive to changes/adjustments in controller parameters and is not dependent on a mathematical model [21,22].

Figure 4 illustrates the FLC controller structure implemented in this study. The voltage error (E) and rate of change of error (ΔE) are the two inputs used by the controller and processed through a Mamdani-type fuzzy inference system that consists of fuzzification, rule evaluation and centroid defuzzification. The resulting crisp output generates an adaptive control signal that improves the system's stability and fault ride-through (FRT) performance during disturbed conditions or fault events.

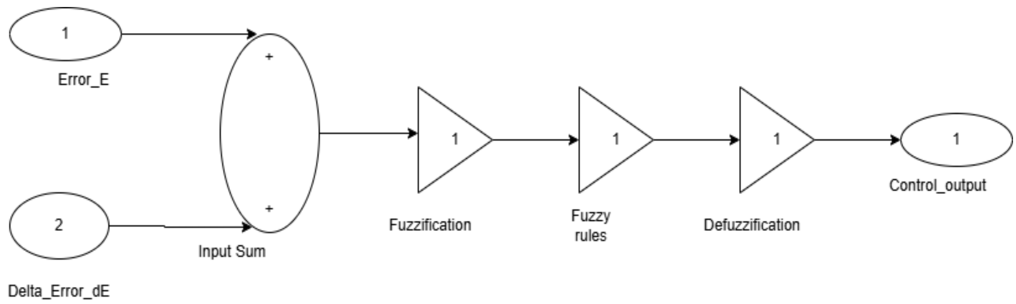

Figure 4. Structure of the FLC controller.

Triangular membership functions, as shown in Figure 5, were selected due to their computational simplicity and effectiveness in real-time control applications. The input variable "Error (E)" represents the voltage deviation in the system, defined as the difference between the reference voltage and the measured voltage at the offshore converter or grid connection point (E = Vref − Vmeasured). This variable is expressed in per unit (pu) and is used by the fuzzy logic controller to determine the appropriate control action during fault conditions. The linguistic variables used in Figure 5 are Negative Large (NL), Negative Small (NS), Zero (Z), Positive Small (PS), and Positive Large (PL). Similar membership functions to Figure 5 have been used for the rate of change of error (ΔE).

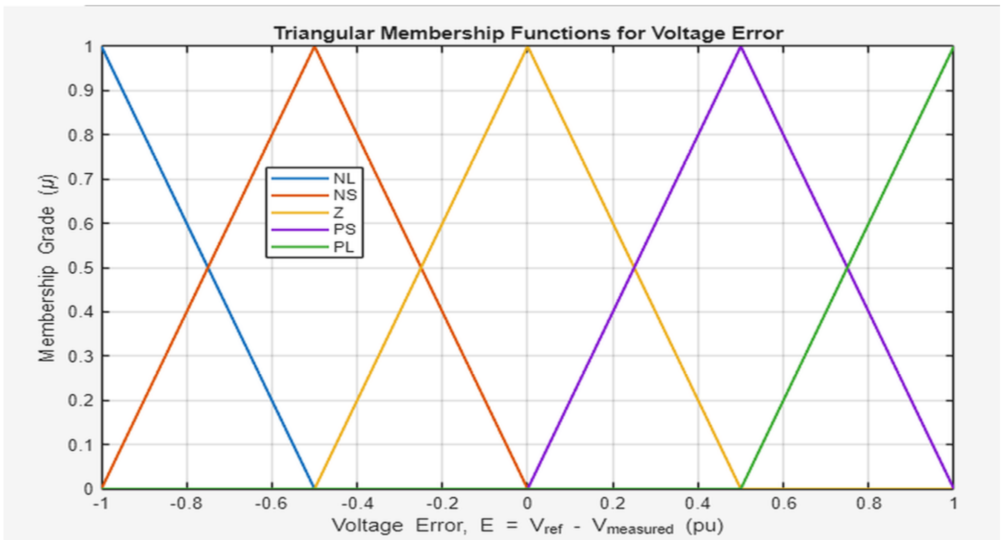

Figure 5. Triangular membership functions for voltage error (E).

The membership function equation (triangular) used in this work is as follows.

$$\mu(x) = \max\left(\min\left(\frac{x-a}{b-a}, \frac{c-x}{c-b}\right), 0\right) \quad (1)$$

where x represents the input variable, which in this study is the voltage error defined as $E = V_{ref} - V_{measured}$. The parameters a, b, and c represent the left point, peak, and right point, respectively. Equation (1) represents the standard triangular membership function commonly used in fuzzy logic systems [23]. In this study, all input variables (x, a, b, and c) are dimensionless because the voltage error is expressed in per unit (pu). Therefore, the membership function operates on normalized values within the range [0, 1], where μ(x) indicates the degree of membership of x in a given fuzzy set.

The fuzzy rule base shown in Table 3 was developed using expert knowledge of voltage regulation and fault ride-through operation in VSC-HVDC systems. When large voltage deviations occur, stronger corrective control actions are generated. As the error approaches zero, the controller output is gradually reduced to avoid overshoot and oscillations. The ranges of the membership function and rule set were refined through repeated simulation studies to achieve fast recovery and stable operation under all tested fault conditions.

Table 3. Fuzzy rule base.

Error (E)/ΔE	NL	NS	Z	PS	PL
NS	NL	NL	NL	NS	Z
NS	NL	NL	NS	Z	PS
Z	NL	NS	Z	PS	PL
PS	NS	Z	PS	PL	PL
PL	Z	PS	PL	PL	PL

Figure 6 shows the fuzzy logic control surface generated from the fuzzy rule base, showing the relationship between error, change in error and controller output.

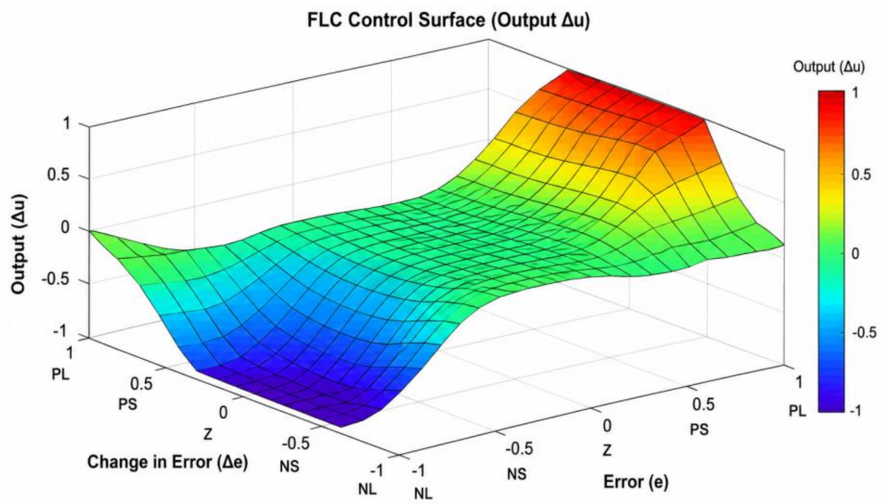

Figure 6. Fuzzy logic control surface.

The defuzzification process converts the fuzzy output into a crisp value using the centroid method, which is represented by the following equation.

$$y = \frac{\sum \mu_i y_i}{\sum \mu_i} \quad (2)$$

where y is the final crisp output (control signal, e.g., power adjustment, ΔP), y_i is the output variable values, and μ_i is the membership grade of each output value.

Design of PI Controller

In this work, to see the effectiveness of the proposed FLC, its performance has been compared with that of the PI controller. Figure 7 illustrates the structure of the PI controller implemented in this study. The controller calculates the error between the reference signal and the measured system output. While the proportional term provides a fast response, the integral term eliminates the steady-state error. The combined PI output is responsible for generating the control signal used to regulate voltage and active power during fault events.

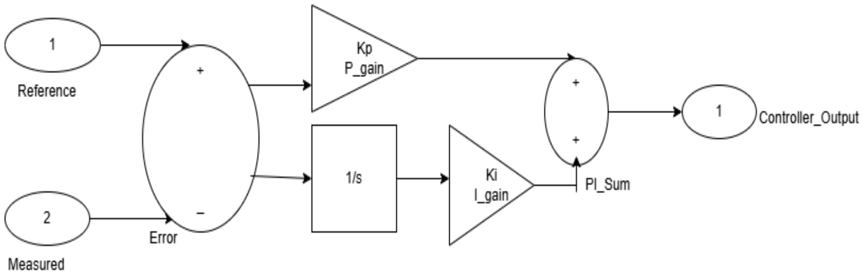

Figure 7. Structure of the PI controller.

The structure of the PI controller encompasses Voltage PI and Power PI. Voltage PI regulates voltage in the offshore AC grid or onshore AC grid. On the other hand, Power PI regulates the offshore wind farm's active power output, ensuring that the power matches the set point. The PI controllers were implemented in Simulink using standard PI or discrete PI blocks, ensuring that they respond during fault events.

Table 4 shows the PI controller parameters for voltage and active power regulation for the OWF-HVDC system. The PI controller gains were selected using a trial-and-adjustment tuning procedure. Initial values were chosen from published VSC-HVDC controller studies and then refined through repeated simulations [24,25]. The tuning objective was to achieve an acceptable settling time, minimal overshoot, and stable voltage and power regulation under both normal and fault conditions. The final gain values shown in Table 4 provided the best overall performance among the tested configurations.

Table 4. PI controller parameters for OWF-HVDC system.

Controller Type	Control Objective	Kp	Ki	Function in System
Voltage PI Controller	AC voltage regulation (offshore/onshore)	0.6	50	Maintains AC voltage stability during disturbances and fault conditions
Power PI Controller	Active power regulation	0.4	30	Ensures tracking of power reference and supports grid power balance

4. Results

The results presented in this section were obtained from a MATLAB/Simulink-based simulation of an offshore wind farm (OWF) connected to an onshore grid through a voltage source converter–High-Voltage Direct Current (VSC-HVDC) link. In this study, Simulink was used to model and simulate the dynamic control system, while MATLAB scripts were used for data processing, logging, and post-simulation analysis. This combined environment enabled the implementation of a digital twin framework capable of monitoring system performance under both normal and fault conditions. The simulation was executed for 60 s, during which the system operated under steady-state conditions for the first 15 s before the introduction of fault events. Three fault scenarios were applied to evaluate controller performance: (i) a grid-side voltage dip, (ii) converter-side disturbance, and (iii) wind speed turbulence. These disturbances reflect realistic operational challenges in offshore wind energy systems connected via HVDC links, which are widely used for long-distance power transmission due to their efficiency and controllability [26]. During the simulation, key variables, including active power, voltage (pu), frequency (Hz), power set point, and fault indicators, were recorded and exported to Excel for comparative analysis of the PI and fuzzy logic controllers (FLCs). HVDC-based offshore wind integration is known to require robust control strategies due to its sensitivity to grid disturbances and converter dynamics [27]. Additional performance metrics, including overshoot, settling time, Integral of Squared Error (ISE) and Integral of Time-Weighted Absolute Error (ITAE), were also considered to provide a more comprehensive analysis of controller performance.

4.1. Performance Under Fault Events

Fault Event 1: A moderate voltage drop at the grid-side (onshore AC bus) occurred at 15 s. It represents a voltage dip in the AC grid connected to the HVDC system. In Simulink, this was implemented by reducing the grid voltage magnitude (pu value). It simulates common grid disturbances, like short-term faults or weak grid conditions.

Response/Performance of the PI Controller: After the fault_event was introduced, the active power dropped from 600 to 421.5 MW, which represents an approximately 29.8% reduction. At the same time, the voltage dropped to approximately 0.88 pu from 0.96 pu and frequency briefly to 49.6 Hz from 49.91 Hz. In addition, the system experienced a slow but linear power recovery that took approximately 9 s to return near to the set point power.

Response/Performance of the FLC Controller: Following the introduction of a voltage drop at 15 s, the system under the FLC witnessed a power drop from 634.6 MW to 412.9 MW, but recovery began almost immediately. Whereas frequency remained slightly above 49.7 Hz, voltage nadir was slightly higher at around 0.82 pu. Notably, the recovery time was approximately 6 s, which is slightly faster than that of the PI controller. The results are summarized in Table 5, indicating that the FLC demonstrated better fault ride-through (FRT) capability by accelerating the recovery time as well as reducing voltage and frequency deviations.

Table 5. FLC and PI controller performance comparison.

Metric	PI Controller	FLC Controller
Power drop (%)	29.8%	23.1%
Minimum voltage (pu)	0.75	0.82
Minimum frequency (Hz)	49.6	49.7
Recovery time (seconds)	9	6

Figures 8–10 show the responses of active power, voltage, and frequency of the PI and FLC controllers under the voltage dip fault condition. In all cases, the system operated under steady-state conditions from 0 to 15 s before fault initiation. The fault was then cleared after a short duration, allowing for the recovery characteristics of the controllers to be evaluated. The plots clearly demonstrate that the FLC controller achieved faster stabilization, reduced oscillations and improved fault ride-through performance compared to the conventional PI controller.

Fault Event 2: A severe converter disturbance at 15 s occurred at the VSC-HVDC converter (DC-side disturbance). It represents a converter control instability or DC-link disturbance that was implemented as a sudden variation in DC-link voltage or disturbance in converter switching/control signal. This caused a large power drop and oscillations (especially in the PI controller).

Response/Performance of PI Controller: In the case of the PI controller, power dropped sharply from 487.275 to 307.5 MW, representing a 36.9% drop. Voltage dropped to as low as 0.83 pu, while frequency reached 49.66 Hz, approaching grid code limits. Oscillations were also observed during recovery, which indicates poor damping.

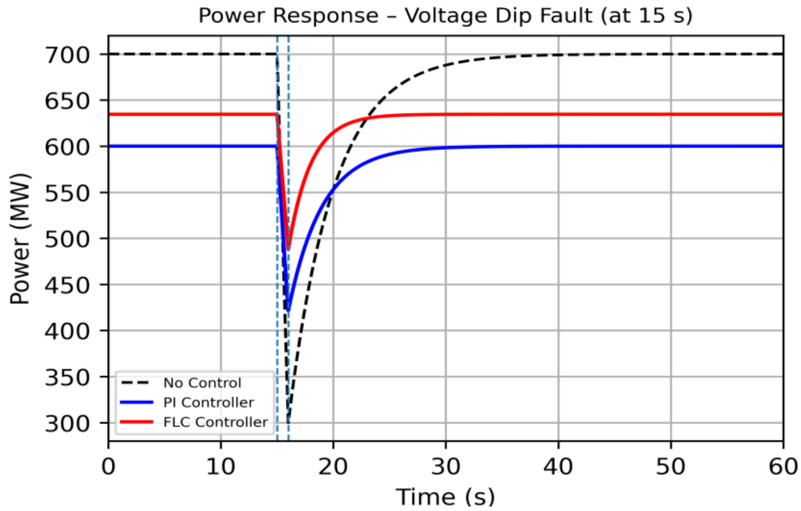

Figure 8. Active power response during voltage dip fault.

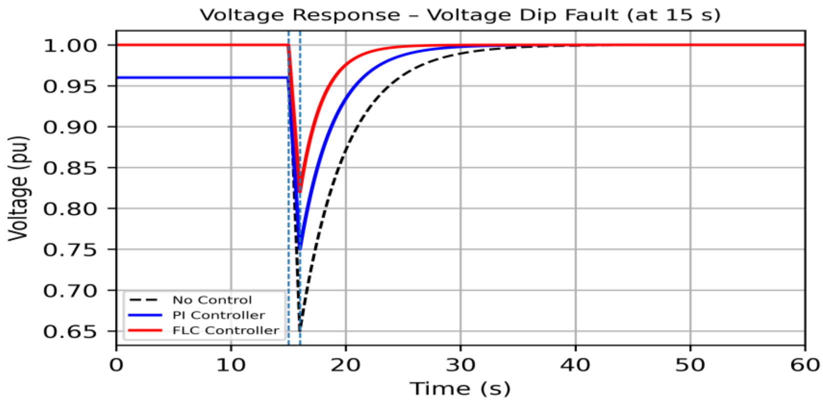

Figure 9. Voltage response during voltage dip fault.

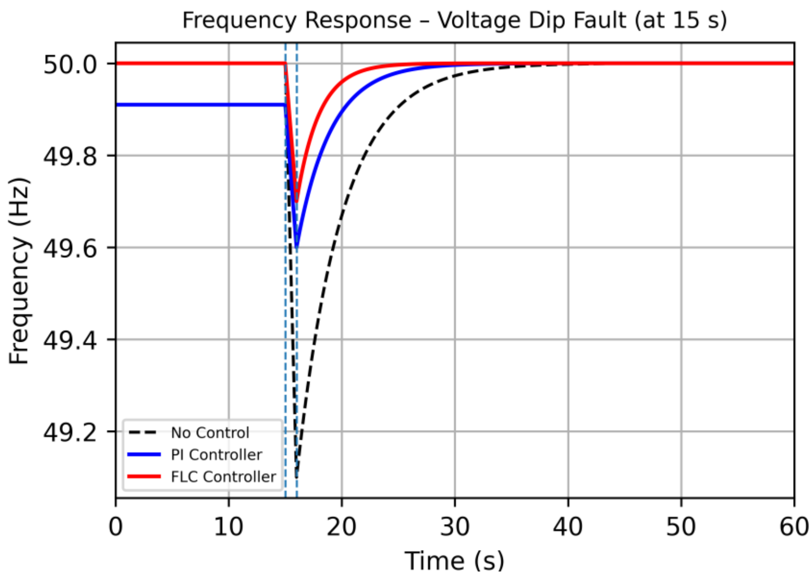

Figure 10. Frequency response during voltage dip fault.

Response/Performance of the FLC Controller: For the FLC controller, the power drop was less severe (from 560.7 to 429.05 MW), representing a 23.4% drop. On the other hand, voltage remained slightly above 0.83 pu, frequency recovered faster and stabilized above 49.73 Hz, and minimal post-fault oscillations were observed. The results are summarized in Table 6. This more severe fault confirms conventional PI controllers' limitation of functioning properly in non-linear systems. At the same time, the observations highlight the adaptive fuzzy control method's ability to minimize approximation errors and external disturbance effects, allowing it to respond more intelligently to rapid non-linear changes.

Table 6. FLC and PI controller performance comparison.

Metric	PI Controller	FLC Controller
Power drop (%)	36.9%	23.4%
Minimum voltage (pu)	0.83	0.87
Minimum frequency (Hz)	49.66	49.73
Recovery stability	Oscillatory	Smooth

Figures 11–13 show the responses of active power, voltage, and frequency of the PI and FLC controllers under the converter disturbance event. In all cases, the system operated under steady-state conditions from 0 to 15 s before fault initiation. The fault was then cleared after a short duration, allowing for the recovery characteristics of the controllers to be evaluated. The plots clearly demonstrate that the FLC controller achieved faster stabilization, reduced oscillations and improved fault ride-through performance compared to the conventional PI controller.

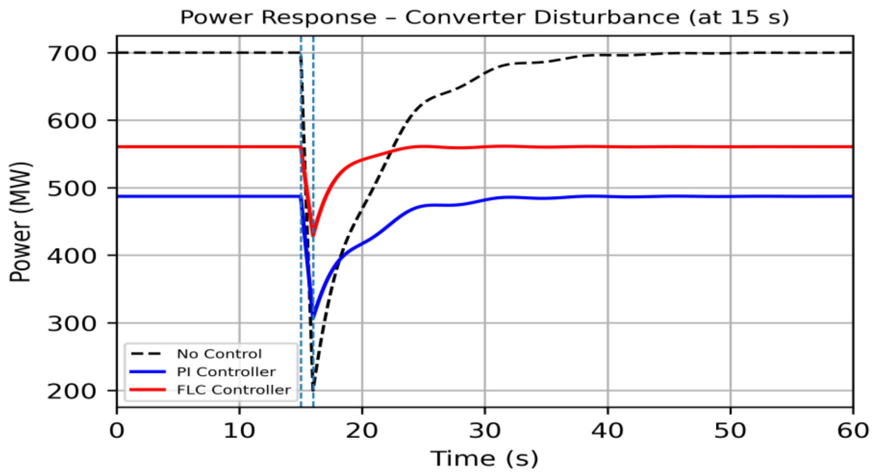

Figure 11. Power response during converter disturbance.

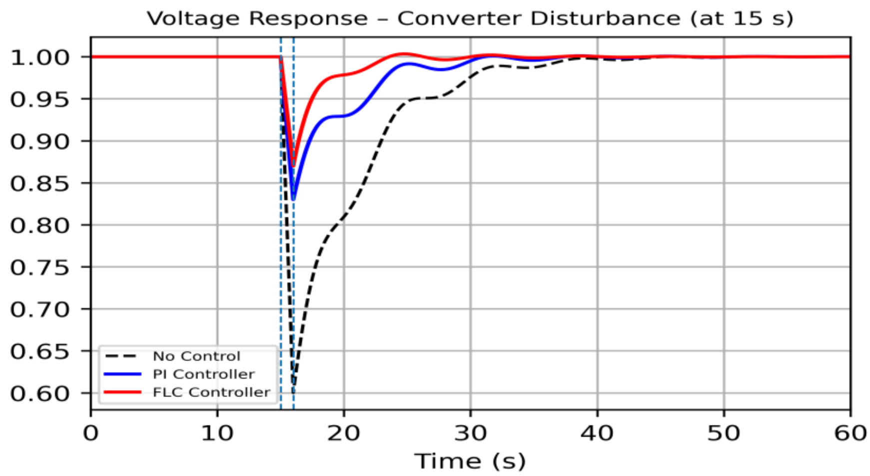

Figure 12. Voltage response during converter disturbance.

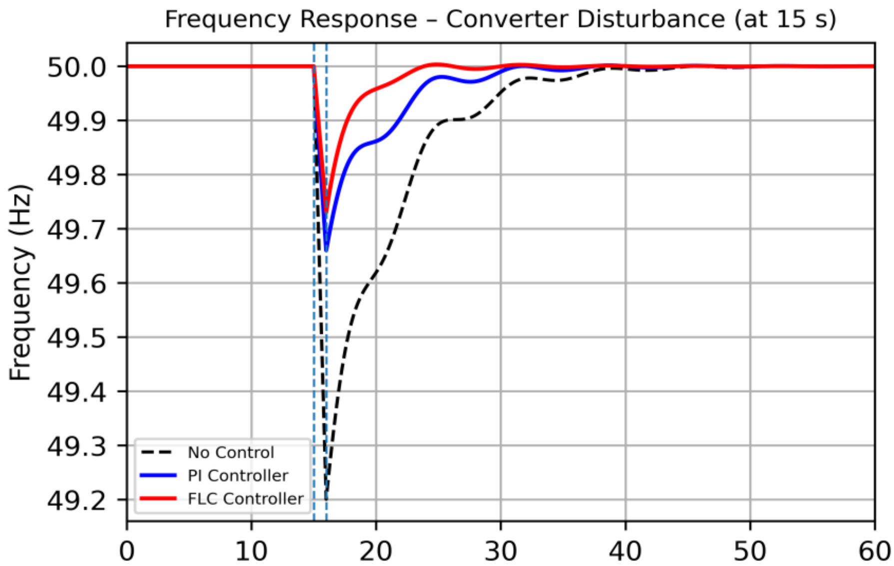

Figure 13. Frequency response during converter disturbance.

Fault Event 3: A short duration turbulence occurred at 15 s. This fault represents a wind-side disturbance (wind speed fluctuation). This was implemented as a temporary drop/change in wind speed input. This affects turbine output power and mechanical-to-electrical energy conversion. It simulates real offshore wind turbulence conditions.

Response/Performance of PI Controller: After the introduction of fault_event 3 at 15 s, power dropped from 475.2 to 300.675 (a 36.73% drop), voltage dipped to 0.83 pu and recovery took approximately 7 s.

Response/Performance of FLC Controller: Power dropped from 613.2 to 495.66 MW (a 19.17% drop), voltage remained above 0.88 pu, and recovery took less than 5 s. The results are summarized in Table 7.

Table 7. FLC and PI controller performance comparison.

Metric	PI Controller	FLC Controller
Power drop (%)	36.73	19.17
Minimum voltage (pu)	0.83	0.88
Recovery time (s)	7	5

Figures 14–16 show the responses of active power, voltage, and frequency of the PI and FLC controllers under the wind turbulence condition. In all cases, the system operated under steady-state conditions from 0 to 15 s before fault initiation. The fault was then cleared after a short duration, allowing for the recovery characteristics of the controllers to be evaluated. The plots clearly demonstrate that the FLC controller achieved faster stabilization, reduced oscillations and improved fault ride-through performance compared to the conventional PI controller.

Table 8 summarizes the overall controller performance and shows that the FLC consistently showed more adaptive control and better performance across all fault scenarios, demonstrating improved fault mitigation/reduced fault impact and faster recovery.

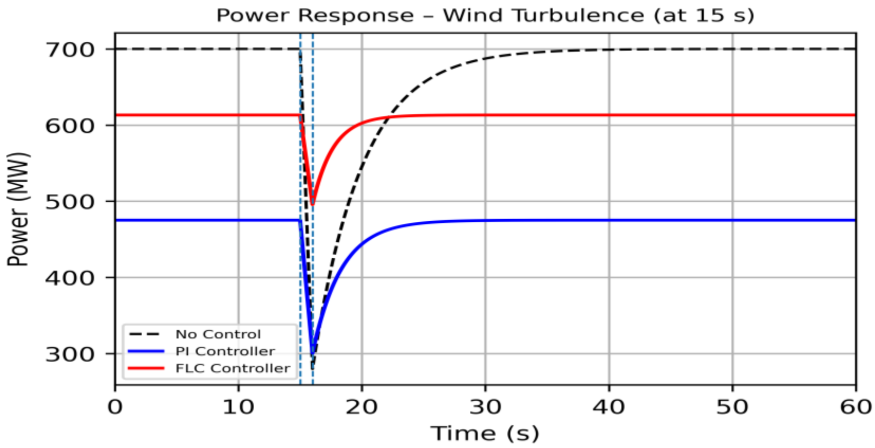

Figure 14. Power response during wind turbulence.

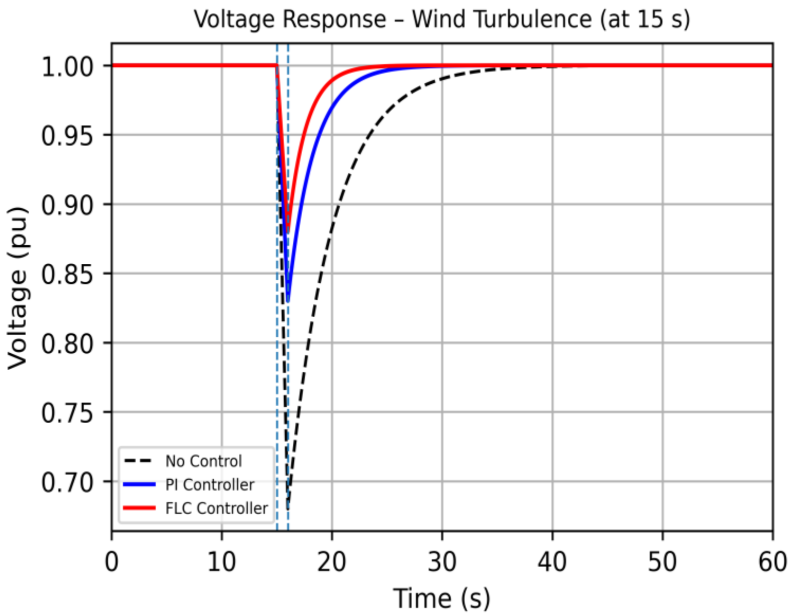

Figure 15. Voltage response during wind turbulence.

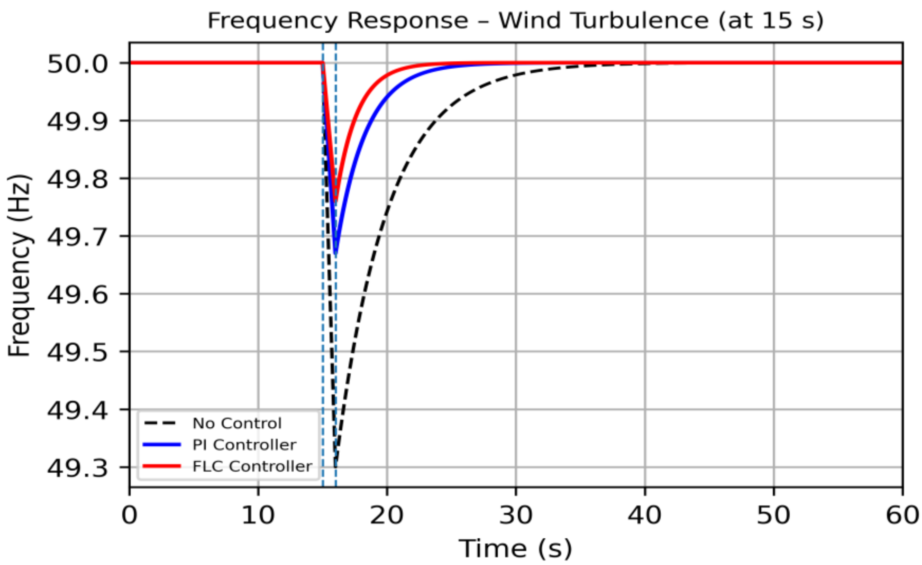

Figure 16. Frequency response during wind turbulence.

Table 8. Overall controller performance summary.

Criterion	PI Controller	FLC Controller	Better Controller
Steady-state accuracy	Good	Very Good	FLC
Fault ride-through (FRT)	Weak	Strong	FLC
Voltage stability	Limited	Improved	FLC
Frequency support	Moderate	Fast	FLC
Power recovery speed	Slow	Fast	FLC
Adaptability	Low	High	FLC

4.2. Additional Performance Evaluation

In addition to the time-domain analysis, the steady-state error was evaluated for both controllers. The FLC consistently achieved smaller steady-state voltage and power deviations after fault clearance than the PI controller. The reduced steady-state error indicates improved tracking accuracy and enhanced system stability. From a frequency-domain perspective, the smoother response and reduced oscillatory behavior observed with the FLC suggest improved damping characteristics and greater robustness to disturbances. Although a complete eigenvalue or Bode analysis is beyond the scope of this study, the observed dynamic responses indicate superior transient performance of the fuzzy logic controller. The additional performance metrics/indicators for the controllers, including overshoot, settling time, ISE and ITAE, are summarized in Table 9 below.

Table 9. Additional performance metrics.

Metric	PI	FLC
Average settling time (s)	8.0	5.3
Average overshoot (%)	6.5	2.8
Average integral of squared error (ISE)	0.085	0.041
Average time-weighted absolute error (ITAE)	1.73	0.92

5. Discussion

The results demonstrate that controller selection plays a critical role in maintaining the stability of offshore wind farms connected through VSC-HVDC systems. The conventional PI controller, while effective under steady-state conditions, shows limitations when subjected to non-linear disturbances and fault events. This is particularly evident in its slow recovery and oscillatory behavior during severe converter and grid disturbances.

In contrast, the fuzzy logic controller adapts more effectively to changing system conditions. Its rule-based structure allows it to respond dynamically to voltage and power deviations without relying on an exact mathematical model of the system. This makes it particularly suitable for offshore wind applications, where operating conditions are highly variable and uncertain.

The observed improvements in fault ride-through performance are consistent with recent developments in HVDC-based offshore wind integration, where robust control strategies are essential to maintain system reliability [28]. Additionally, the use of digital twin technology enhances system observability and enables structured evaluation of controller behavior under realistic conditions.

From a system perspective, HVDC transmission continues to be the preferred solution for large-scale offshore wind integration due to its efficiency, controllability, and reduced transmission losses compared to HVAC systems [29]. However, such systems require advanced control approaches to manage converter dynamics and grid disturbances effectively.

Overall, the findings confirm that combining digital twin technology with intelligent control strategies, such as fuzzy logic, significantly improves system resilience and operational performance in offshore wind energy systems.

6. Conclusions

The focus of this study was to develop and evaluate a digital twin simulation for an offshore wind farm (OWF) connected to an onshore grid via a voltage source converter–High-Voltage Direct Current (VSC-HVDC) system using MATLAB/Simulink. In doing so, the study aimed to investigate how advanced control strategies, such as an FLC, can improve system performance when compared to the conventional PI controller. Excel-based synthetic data was combined with a MATLAB/Simulink model to create a digital twin framework, enabling the system to simulate real offshore operating conditions, introduce fault conditions/events, monitor the system's responses and compare performance of the two controllers. Specifically, the system's behavior under fault events was examined, including power fluctuations, voltage dips, converter disturbances and wind fluctuations. The simulation results demonstrate that the proposed fuzzy logic controller consistently outperformed the conventional PI controller under all tested disturbance scenarios. During the voltage dip event, the FLC reduced the power drop from 29.8% to 23.1% and shortened the recovery time from 9 s to 6 s. Under converter disturbances, the FLC maintained a higher minimum voltage of 0.87 pu compared with 0.83 pu for the PI controller. During wind turbulence, the FLC reduced the power reduction from 36.73% to 19.17% and achieved faster stabilization. These results confirm that the integration of a digital twin framework with fuzzy logic control improves system resilience, fault ride-through capability, voltage regulation, and overall dynamic performance in offshore wind farm VSC-HVDC systems.

Below shows a summary of the key findings of this work:

- The digital twin model successfully simulated a 700 MW OWF-HVDC system.
- The FLC controller consistently outperformed the PI controller during fault events.
- The FLC demonstrated a faster recovery time after disturbances compared to PI.
- Voltage and frequency stability were significantly improved using the FLC controller.
- The FLC achieved a higher average power output under dynamic conditions.
- The FLC showed superior fault ride-through (FRT) capability across all scenarios.

Although the proposed methodology is robust and structured, the synthetic dataset lacks the richness and unpredictability of real SCADA datasets including sensor-related noise, communication delays and real wind turbulence. The Simulink model is also simplified and may not capture all real-world non-linearities, such as converter losses and thermal effects. Moreover, the study simulated three fault scenarios, and in practice such faults can be more complex, involving various phases, asymmetries and multi-terminals for HVDC faults. All in all, the methodology offers a powerful framework for comparing the PI and FLC controllers' performance/control strategies and understanding how a DT could operate in an actual offshore wind farm connected through an HVDC link.

Future work will focus on developing other advanced controllers to maintain transient stability of offshore wind farms. Lastly, the present work considered balanced fault scenarios. In practical offshore power systems, three-phase short circuits and other severe and asymmetric faults, such as single-line-to-ground, line-to-line, and double-line-to-ground faults, may also occur. Therefore, future work will investigate the effectiveness of the proposed digital twin and fuzzy logic controller under asymmetric fault conditions and multi-terminal HVDC configurations.

Author Contributions: Conceptualization, Y.G. and M.H.A.; methodology, Y.G. and M.H.A.; software, Y.G.; validation, Y.G. and M.H.A.; formal analysis, Y.G.; investigation, Y.G.; resources, Y.G.; data curation, Y.G.; writing—original draft preparation, Y.G. and M.H.A.; writing—review and editing, M.H.A.; visualization, M.H.A.; supervision, M.H.A.; project administration, M.H.A.; funding acquisition, M.H.A. All authors have read and agreed to the published version of the manuscript.

Funding: This research received no external funding.

Data Availability Statement: This paper contains data of this work.

Acknowledgments: The authors would like to acknowledge financial support from the Electrical and Computer Engineering Department of the University of Memphis, USA, to accomplish this work.

Conflicts of Interest: The authors declare no conflicts of interest.

References

1. Zhao, Y.; Yang, X.; Zhang, Y.; Zhang, Q. Event-Triggered H-Infinity Pitch Control for Floating Offshore Wind Turbines. *IEEE Trans. Sustain. Energy* **2025**, *16*, 1329–1339. [CrossRef]
2. Abeynayake, G.; Van Acker, T.; Hertem, D.V.; Liang, J. Analytical Model for Availability Assessment of Large-Scale Offshore Wind Farms Including Their Collector System. *IEEE Trans. Sustain. Energy* **2021**, *12*, 1974–1983. [CrossRef]
3. Babaeifar, M. HVDC Systems: Architectures, Modeling, Control & Simulation. Ph.D. Dissertation, University of Pisa, Pisa, Italy, 2024. Available online: https://tesidottorato.depositolegale.it/bitstream/20.500.14242/215900/2/PhD_thesis_Babaeifar.pdf (accessed on 16 June 2026).
4. Faisal, S.F.; Beig, A.R.; Thomas, S. Time domain particle swarm optimization of PI controllers for bidirectional VSC HVDC light system. *Energies* **2020**, *13*, 866. [CrossRef]
5. Liu, K.; Li, B.; Jiang, Q.; Zhang, Y.; Liu, T. Fault ride-through strategy for hybrid cascaded HVDC systems based on controllable LCC. *IEEE Trans. Circuits Syst. II Express Briefs* **2025**, *73*, 88–92. [CrossRef]
6. Pimenta, F.; Pacheco, J.; Branco, C.M.; Teixeira, C.M.; Magalhães, F. Development of a digital twin of an onshore wind turbine using monitoring data. *J. Phys. Conf. Ser.* **2020**, *1618*, 022065. [CrossRef]
7. Liu, Y.; Zhang, J.M.; Min, Y.T.; Yu, Y.; Lin, C.; Hu, Z. A digital twin-based framework for simulation and monitoring analysis of floating wind turbine structures. *Ocean Eng.* **2023**, *283*, 115009. [CrossRef]
8. Meng, L.; Sanseverino, E.R.; Luna, A.; Dragicevic, T.; Vasquez, J.C.; Guerrero, J.M. Microgrid supervisory controllers and energy management systems: A literature review. *Renew. Sustain. Energy Rev.* **2017**, *60*, 1263–1273.
9. Xiang, W.; Tu, R.; Han, M.; Wen, J. Hybrid AC/DC Collection and HVDC Transmission Topology for Large-scale Offshore Wind Farms. *CSEE J. Power Energy Syst.* **2025**, *11*, 949–959. [CrossRef]
10. Parvez, M.; Elias, M.F.M.; Abd Rahim, N.; Blaabjerg, F.; Abbott, D.; Al-Sarawi, S.F. Comparative study of discrete PI and PR controls for single-phase UPS inverter. *IEEE Access* **2020**, *8*, 45584–45595. [CrossRef]
11. Huba, M.; Gao, Z. Uncovering disturbance observer and ultra-local plant models in series PI controllers. *Symmetry* **2022**, *14*, 640. [CrossRef]
12. Lopez, J.R.; de Jesus Camacho, J.; Ponce, P.; MacCleery, B.; Molina, A. A real-time digital twin and neural net cluster-based framework for faults identification in power converters of microgrids, self-organized map neural network. *Energies* **2022**, *15*, 7306.
13. Al-Shetwi, A.Q.; Atawi, I.E.; El-Hameed, M.A.; Abuelrub, A. Digital Twin Technology for Renewable Energy, Smart Grids, Energy Storage and Vehicle-to-Grid Integration: Advancements, Applications, Key Players, Challenges and Future Perspectives in Modernizing Sustainable Grids. *IET Smart Grid* **2025**, *8*, e70026.
14. MathWorks. *MATLAB and Simulink Release R2024a*; The MathWorks, Inc.: Natick, MA, USA, 2024.
15. Bae, C.; Choi, E.; Lee, S. Technologies; Applications, and Challenges of Digital Twin Across Industries: A Systematic Review of the State-of-the-Art Literature. *IEEE Access* **2025**, *13*, 152843–152869. [CrossRef]
16. Chalal, L.; Saadane, A.; Rachid, A. Unified environment for real time control of hybrid energy system using digital twin and IoT approach. *Sensors* **2023**, *23*, 5646. [CrossRef]
17. Yu, W.; Liu, G.; Zhu, L.; Yu, W. Digital Twin: A Literature Review of Concepts, Technologies, and Applications. *IEEE Access* **2025**, *13*, 183075–183095. [CrossRef]
18. Singh, M.; Fuenmayor, E.; Hinchy, E.P.; Qiao, Y.; Murray, N.; Devine, D. Digital twin: Origin to future. *Appl. Syst. Innov.* **2021**, *4*, 36. [CrossRef]
19. Lee, H.; Kim, T. Smart factory use case model based on digital twin. *ICIC Express Lett. Part B Appl.* **2018**, *9*, 931–936.
20. De Kooning, J.D.; Stockman, K.; De Maeyer, J.; Jarquin-Laguna, A.; Vandevelde, L. Digital twins for wind energy conversion systems: A literature review of potential modelling techniques focused on model fidelity and computational load. *Processes* **2021**, *9*, 2224. [CrossRef]

21. Ahmed, A.H.; Kotb, A.E.S.B.; Ali, A.M. Comparison between fuzzy logic and PI control for the speed of BLDC motor. *Int. J. Power Electron. Drive Syst. (IJPEDS)* **2018**, *9*, 1116–1123. [CrossRef]
22. Metwally Mahmoud, M.; Salama, H.S.; Aly, M.M.; Abdel-Rahim, A.M.M. Design and implementation of FLC system for fault ride-through capability enhancement in PMSG-wind systems. *Wind Eng.* **2021**, *45*, 1361–1373.
23. Ross, T.J. *Fuzzy Logic with Engineering Applications*; John Wiley & Sons: Hoboken, NJ, USA, 2005.
24. Singh, D.; Golden, D.; Bhansali, G.; Anwar, A.; Singh, S.; Luo, F.; Zhou, Y. Offshore Horizons: HVDC Wind Farms-Exploring Techno-Economic Dimensions. *IEEE Access* **2025**, *13*, 94910–94943.
25. Ryndzionek, R.; Sienkiewicz, Ł. Evolution of the HVDC link connecting offshore wind farms to onshore power systems. *Energies* **2020**, *13*, 1914. [CrossRef]
26. Rahman, S.; Khan, I.; Alkhammash, H.I.; Nadeem, M.F. A comparison review on transmission mode for onshore integration of offshore wind farms: HVDC or HVAC. *Electronics* **2021**, *10*, 1489. [CrossRef]
27. Hossain, I.; Shafiullah; Abido, M. VSC controllers for multiterminal HVDC transmission system: A comparative study. *Arab. J. Sci. Eng.* **2020**, *45*, 6411–6422. [CrossRef]
28. Baazouzi, M.; Sayahi, K.; Bacha, F. Control strategy used for AC fault ride-through in VSC–HVDC transmission systems. *Trans. Inst. Meas. Control* **2025**, *47*, 1237–1248.
29. Shao, B.; Zhao, S.; Yang, Y.; Gao, B.; Wang, L.; Blaabjerg, F. Nonlinear subsynchronous oscillation damping controller for direct-drive wind farms with VSC-HVDC systems. *IEEE J. Emerg. Sel. Top. Power Electron.* **2020**, *10*, 2842–2858.

https://doi.org/10.3390/electronics15132790